6th ECCOMAS Conference on Smart Structures and Materials
SMART2013
Politecnico di Torino, 24-26 June 2013
E. Carrera, F. Miglioretti and M. Petrolo (Editors)
www.smart2013.com

THERMAL EFFECTS ON THE TORQUE CHARACTERISTICS OF A MAGNETORHEOLOGICAL CLUTCH

Francesco Bucchi, Paola Forte, Francesco Frendo

University of Pisa
Department of Civil and Industrial Engineering
Largo Lucio Lazzarino
56126, Pisa, Italy
e-mail: frendo@ing.unipi.it

Key words: Magnetorheological fluids, MR, magnetorheological clutch, experimental characterization, temperature, thermal dependence, automotive application.

Summary. *The temperature dependence of the properties of magnetorheological fluids has been already considered in the literature, but such an aspect related to MR clutches/brakes has not yet been analysed, though thermal effects on torque proved to be significant.*
In this paper the torque characteristic of a permanent magnet magnetorheological clutch is investigated focusing on the influence of temperature. An experimental campaign was carried out on a test bench equipped with a caulk heating up to 80^o C. The torque characteristics were measured and both the fluid and the clutch case temperature were monitored at the beginning and at the end of each test.
Torque data were processed and well fitted by a formula where the temperature dependence is expressed by Arrhenius law, taking into account the temperature variation during the test. In particular a loss of transmitted torque for increasing temperature was found.
The dependence of the gap average shear stress on temperature was also approximately estimated on the basis of finite element magnetic analyses and simplifying assumptions which could be used to estimate torque-temperature dependence on similar devices.

1. INTRODUCTION

Magnetorheological fluids (MR fluids) are smart materials which exhibit changes in their rheological properties as a function of the magnetic field which are subjected to. The main applications of MR fluids are dampers, in automotive and civil fields, due to the capability of changing the apparent viscosity as a function of the magnetic field generated by coils or permanent magnets. They are also used in clutches and brakes due to their viscoplastic behaviour where the yield stress value increases with the magnetic field. Several mechanical models have been developed to reproduce the fluid characteristic, starting from the Bingham-plastic (BP) and Herschel-Bulkley up to more accurate ones. However most of these models express the

shear stress of the fluid as a function of only the magnetic field H and shear-rate $\dot{\gamma}$, neglecting thermal effects

$$\tau = \tau(H, \dot{\gamma}). \tag{1}$$

Only recently some authors investigated the effects of the temperature on MR fluids and elastomers. In [1] the apparent viscosity in MR dampers was studied as a function of the magnetic field and temperature by means of a shear rate controlled rheometer. Arrhenius equation was used to fit results which showed the decrease of viscosity with rising temperature. In [2] the rheological properties of an in-house developed fluid were investigated with relation to the magnetic field and temperature. Data were fitted according to power law models [3]. In addition to MR fluids, also MR grease temperature properties were investigated in [4] and [5] revealing a decrease of viscosity as the temperature increases. In particular in [4] the complex modulus of the fluids is investigated as a function of temperature.

As far as the effects of temperature on MR devices are concerned, the published papers are even fewer. In [6] they were considered in the analysis of the behaviour of magnetorheological dampers while in [7] they were taken into account in the development of a controlled magnetorheological brake.

During a preliminary characterization of an MR clutch [8, 9] the authors observed an apparent relationship between the torque characteristic of the engaged clutch and the self produced heat due to the clutch slip. In particular a loss of torque was experienced as the dissipated work increased, which reduced the maximum transmissible torque. Therefore considering temperature effects in MR device development appears mandatory.

In this paper the torque characteristic of the above mentioned magnetorheological device is investigated focusing on the influence of temperature. An experimental campaign was carried out on a test bench [10] specifically equipped with a caulk oven able to heat the clutch working environment up to 80 ^{o}C. The torque characteristics were measured by a torquemeter and acquired as a function of the speed difference between the primary and secondary clutch parts and the environment initial temperature. Both the fluid temperature and the clutch case temperature were monitored at the beginning and at the end of each test.

2. MR CLUTCH DESIGN

A fail-safe MR clutch with permanent magnet was developed as a result of a multidisciplinary research. The clutch was designed on the basis of the BP model which relates the shear stress τ, function of the magnetic field H, to the shear rate $\dot{\gamma}$, as shown in Eq. 2

$$\tau(H) = \tau_0(H) + \eta\dot{\gamma} \tag{2}$$

where $\tau_0(H)$ is the yield stress which has to be overcome to have slip and η is the fluid viscosity. The numeric value of τ_0 and η were supplied by the fluid manufacturer, Lord Corporation Ltd .

The magnetic field distribution within the fluid was obtained by finite element magnetic simulations [11] and the torque transmitted by the clutch was predicted on the basis of the

rheological and geometrical properties [12].

The clutch design was driven in order to satisfy the specifications stated in Table 1. The

Table 1. Clutch specifications.

Diameter (mm)	< 70
Length (mm)	< 50
Max Torque Engaged (Nm)	2.5
Nominal Engaged Torque (Nm)	1.0
Disengaged Torque (Nm)	0.5
Max Speed (rpm)	2000

dimensions were established on the basis of the operating room. The values of torque in engaged condition were defined by the necessity of starting (max torque) and keeping in rotation (working torque) a vacuum pump used in a Diesel engine [13]. The clutch torque in disengaged condition had to be as low as possible in order to reduce power loss when the vacuum pump operation is not necessary. The maximum speed descends from the maximum speed of the cam shaft which drives the clutch and the vacuum pump.

Figure 1 shows the clutch prototype draft.

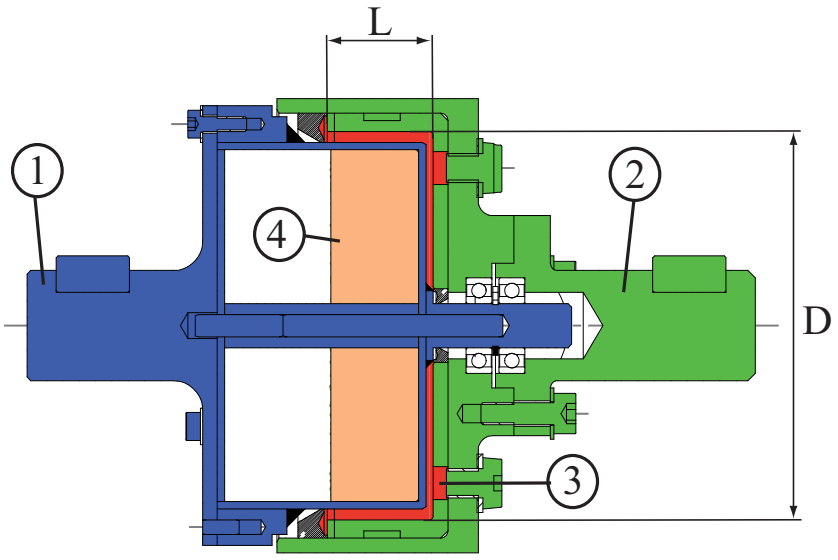

Figure 1. Design of the prototype.

The clutch is composed by the primary (1) and secondary (2) groups, the MR-fluid gap (3) and a sliding NdFeB permanent magnet (4). To engage the clutch the magnet is moved close to the fluid (on the right in Fig. 1), whereas to disengage it is moved on the opposite side (on the left in Fig. 1).

Materials were chosen on the basis of finite element simulations in order to optimize the magnetic field distribution in the engaged condition and to shield the magnet in the disengaged one. The permanent magnet has 4 diametrically magnetized poles. The average value of the magnetic field in the fluid in the engaged condition is about 0.6 T, whereas it results umagnetized when the clutch is disengaged.

3. EXPERIMENTAL ACTIVITY

3.1 Room temperature characterization

An experimental test bench (Fig. 2) was set up to characterize the clutch torque. The brush-

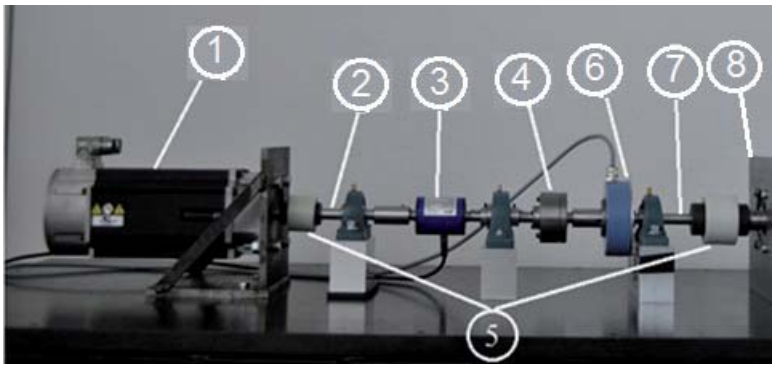

Figure 2. Experimental test bench.

less motor (1) is connected to the primary group of the clutch (4) and controls the speed. The secondary group is kept fixed by a flange (8). The torque is measured by the torquemeter (3) and the speed of the primary group is measured by an encoder embedded in the brushless motor.

A PC endowed with an Input/Output DAQ and a specifically developed program controls the brushless speed and acquires the primary speed and the torque. During the preliminary tests, a dependence of the engaged torque characteristic on the imposed speed law was found. In particular a power time law was imposed to the primary speed, starting from 0 rpm up to the maximum speed which was fixed at 1500 rpm, as shown in Fig. 3.

The power law was chosen in order to accurately identify the yield torque, thanks to the low speed rate at low speed. Figure 4 shows the torque profile obtained imposing the speed profile shown in Fig. 3, starting from environmental temperature $T \simeq 20^{o}$ C. The total length of the test was 20 s. The yield torque was 2.2 Nm which is lower than the maximum torque required by specification (Tab. 3) but is greater than the operating torque; the maximum torque transmitted by the clutch is about 3.4 Nm. Therefore at the engine start-up, due to low temperature and to the accumulation of oil in the vacuum pump, a clutch slip may occur, whereas, once reached the steady state, the clutch will result engaged.

In addition to the test procedure shown in Fig. 3, a new speed profile was introduced to simulate also the engaging phase of the clutch. Once the maximum was reached, the speed was

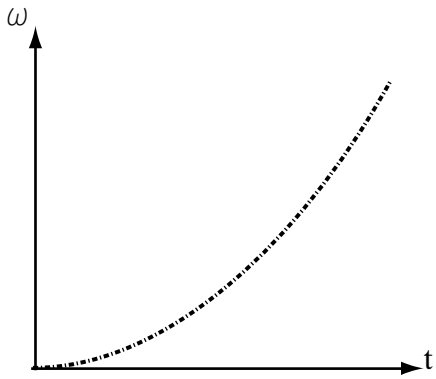

Figure 3. Power-law speed profile.

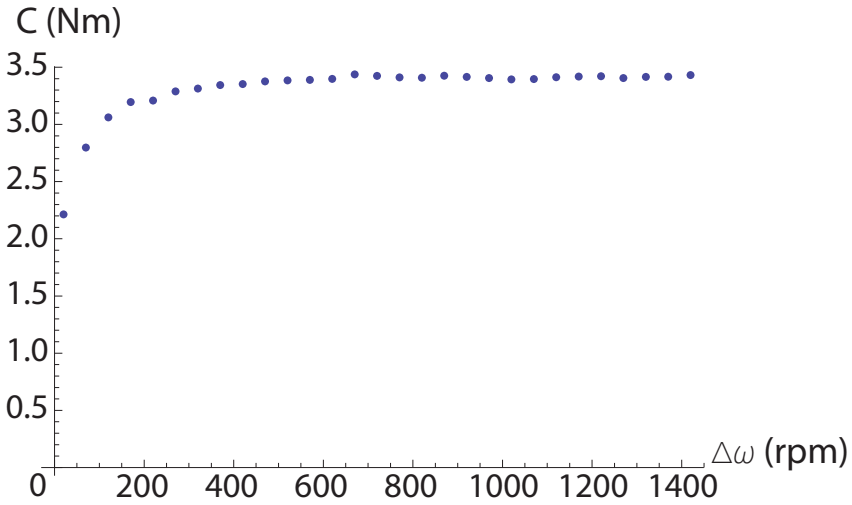

Figure 4. Torque profile at 20º C.

kept constant for 5 s and then the power ramp was inverted and a speed decrease was imposed, as shown in Fig. 5.

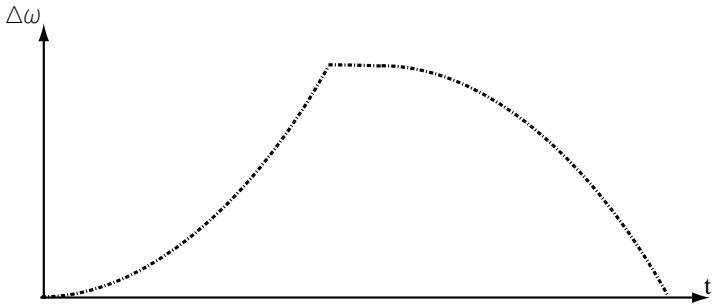

Figure 5. Testing procedure 2.

Figure 6 shows the torque profile obtained. The rising part is comparable to the one obtained

in Fig. 4. During the constant speed part the torque decreases and then, during the decelerating phase, the torque results lower than the previous one.

The loss in the transmitted torque can't be explained by any classical model so an analysis of the clutch torque behaviour was conducted at different environmental temperatures.

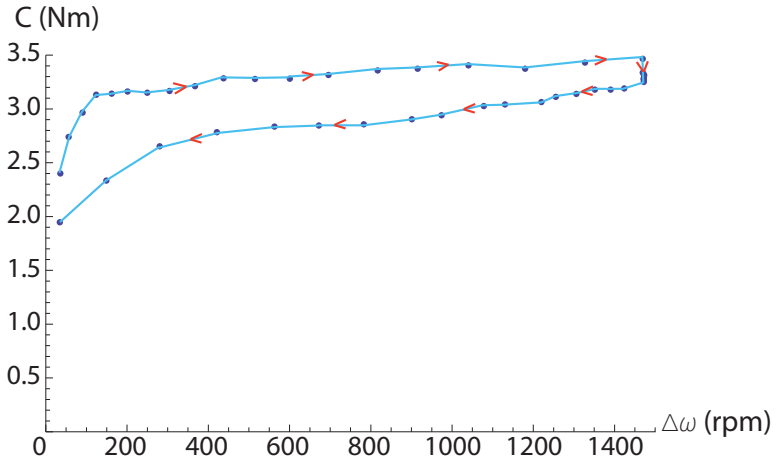

Figure 6. Torque profile at 20° C following the testing procedure 2.

3.2 Tests carried out at different temperatures

The test bench described above was equipped with a caulk oven which can warm the environment sorrounding the clutch. As shown in Fig. 9 the caulk environment is warmed up by four heating elements supplied by an adjustable AC transformer and the case is caulk by mineral wool and refractory tape.

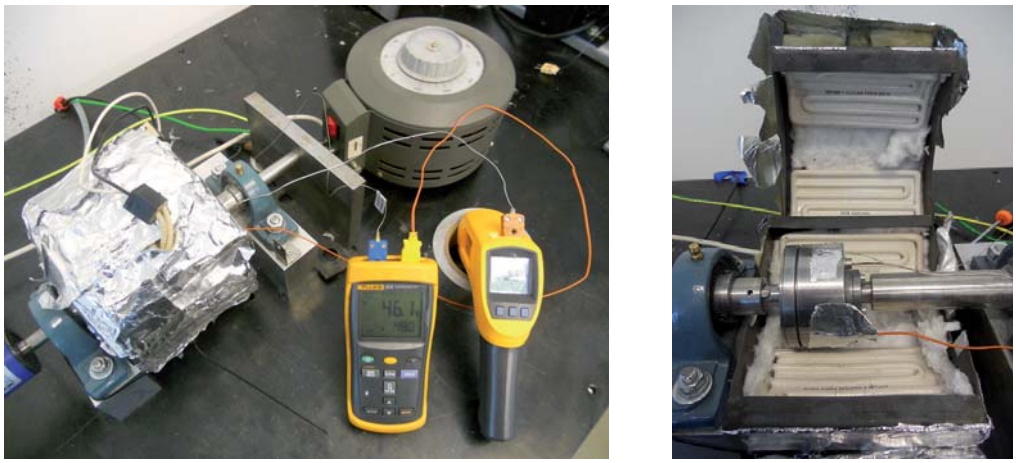

Figure 7. External and internal view of the oven.

Three thermocouples were used to measure the temperature. Two thermocouples (TC1 and TC2) were secured on the external case of the clutch and one thermocouple (TC3) was included coaxially in the screw cap of the MR fluid, in order to measure the fluid temperature. A schematic view of the thermocouples positioning is shown in Fig. 8, whereas the real positioning on the tested prototype is shown in Fig 9. The temperature was displayed on two thermocouple readers.

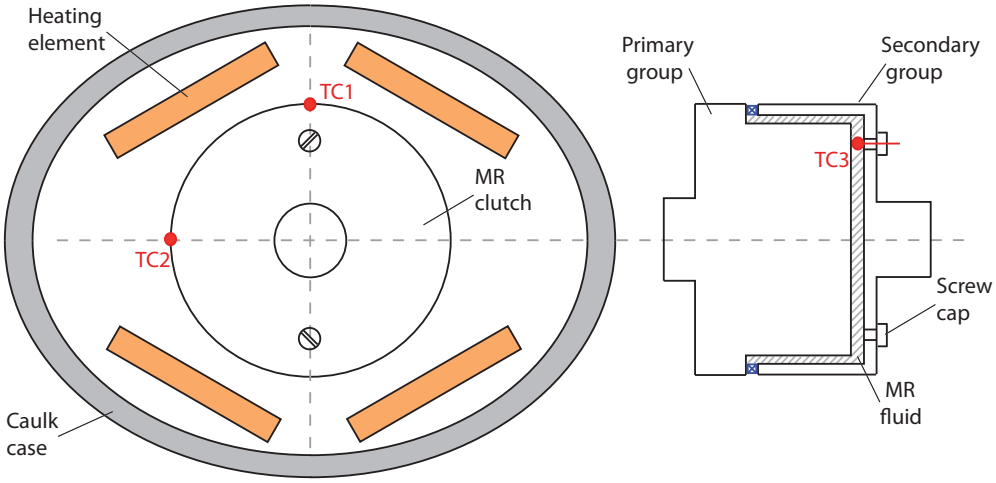

Figure 8. Schematic frontal view of the oven and lateral view of the clutch.

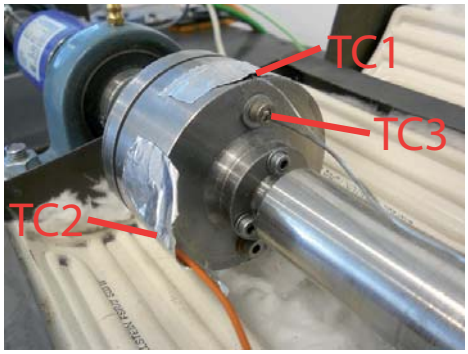

Figure 9. Thermocouple positioning.

By means of the AC transformer the heating elements were slowly heated up to the average value of the temperature read by TC1 and TC2 that was about 5°C greater than the desired environmental temperature. Then the power supply was switched off to let the temperature level into the whole oven room. Once the desired value of temperature was read on the thermocouple reader the test was started.

The speed of the primary shaft was imposed following the profile shown in Fig.3. The torque measured by the torquemeter and the primary shaft speed measured by the encoder were acquired at 100Hz. The tests were conducted starting from six different initial temperatures

(20°C , 30°C , 40°C , 50°C , 60°C , 80°C) and three tests were repeated for each temperature value. In addition the temperature was measured 30s after the end of each test, when the steady temperature value was reached and the thermocouple transient could be neglected. Table 2 summarizes the acquired temperature values.

Table 2. Acquired temperatures.

	Initial			Final		
Reference T (°C)	TC1 (°C)	TC2 (°C)	TC3 (°C)	TC1 (°C)	TC2 (°C)	TC3 (°C)
20	21	21	21	41	41	38
20	22	22	22	41	40	38
20	22	22	22	41	40	39
30	30	30	30	47	46	44
30	32	31	32	47	46	46
30	32	31	32	50	48	47
40	42	42	43	58	56	56
40	42	41	42	60	58	58
40	43	42	43	59	56	57
50	52	51	50	68	67	63
50	52	51	52	67	65	65
50	50	49	51	65	62	64
60	62	61	60	73	71	71
60	62	60	62	76	73	74
60	60	58	61	75	70	73
80	84	82	82	97	93	93
80	81	77	81	94	89	92
80	81	77	82	94	88	92

For each test, the initial values of the temperature are similar in correspondence of the three thermocouples, proving a uniform temperature distribution within the oven. In particular the difference between the higher and lower read values never results more than 5%. Similarly at the end of each test the temperature distribution is fairly uniform.

4. EXPERIMENTAL RESULTS AND FITTING

The raw acquired data were filtered by a moving average (100 samples) to reduce electromagnetic noise and are plotted in Fig. 10. The influence of the initial temperature is clear and produces an almost constant loss in the transmitted torque of about 0.8Nm over the whole examined speed range.

In order to identify more specifically the temperature dependence, the average value of the measured torque was calculated for the tests conducted at the same temperature. Figure 11 shows the averaged results. The differences between lower and higher starting temperature

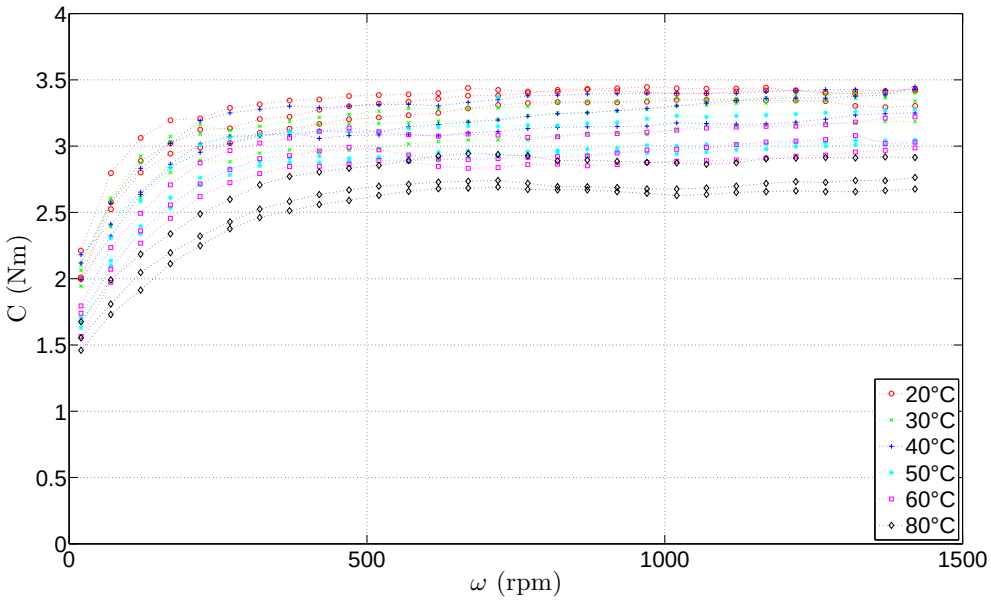

Figure 10. Acquired torque data.

result remarkable, whereas the difference between two next temperature values (e.g. 30^o C and 40^o C) are comparable with the measurement error.

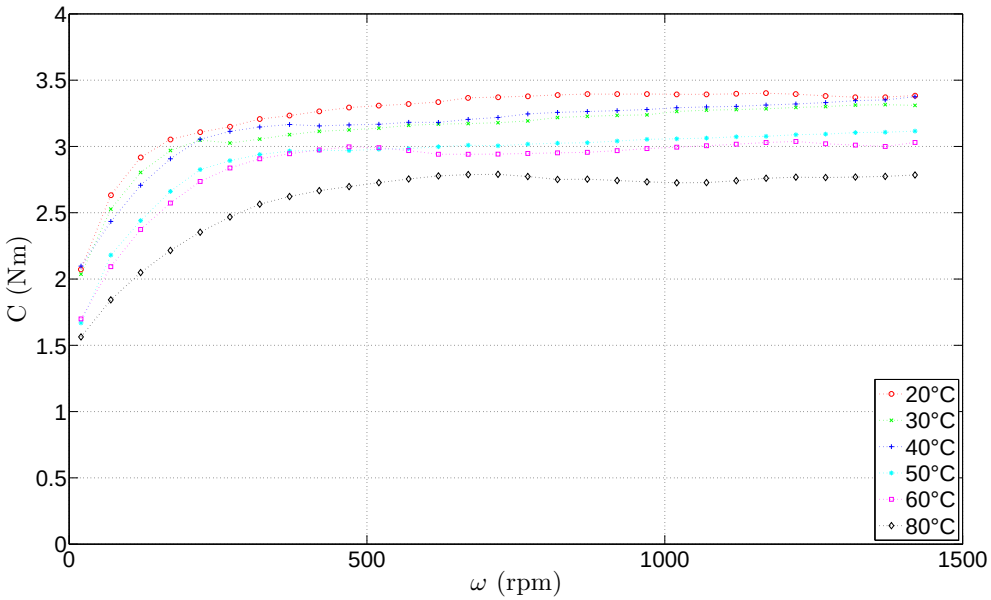

Figure 11. Averaged torque data.

The surface interpolating the average data set is shown in Fig. 12.

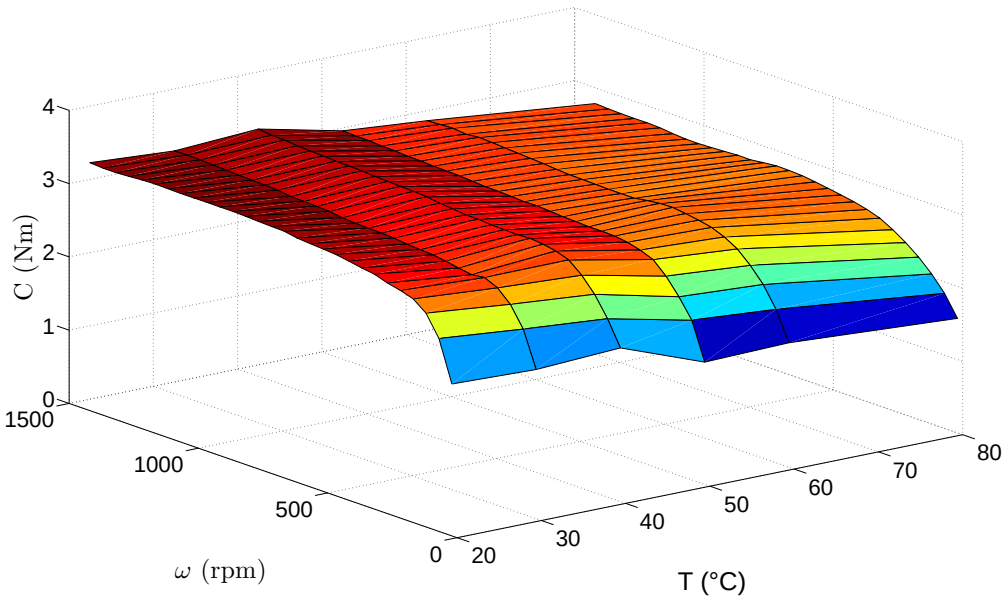

Figure 12. Torque interpolating surface.

The average torque data set shown in Fig 11 was used to find a fitting surface which could match the relationship $C(\Delta\omega, T)$. In particular, on the basis of [3, 5], a formulation composed of a power law to represent the relationship $C(\Delta\omega)$ and the Arrhenius law to express the dependence $C(T)$ was chosen as follows

$$C(\Delta\omega, T) = A\Delta\omega^n e^{-\frac{B}{T}} \tag{3}$$

where $\Delta\omega$ and T are the speed difference and initial temperature (measured in K) considered in the data set, C is the torque computed as the mean of the acquired torque values in correspondence of given $\Delta\omega$ and T and A, B and n are the parameters to be determined by the fitting technique.

The *MatLab Curve Fitting Tool* was used to obtain the parameters values listed in Tab. 3 which, if included in the Eq. 3, give the surface represented in Fig. 13.

Table 3. Fitting parameters.

A (Nm/rpm^n)	0.5227
n	0.09611
B (K^{-1})	360.5

The R-square value computed for the fitting was 0.8793. In order to improve the goodness of fit, the acquired average data were manipulated considering the fluid warming during each

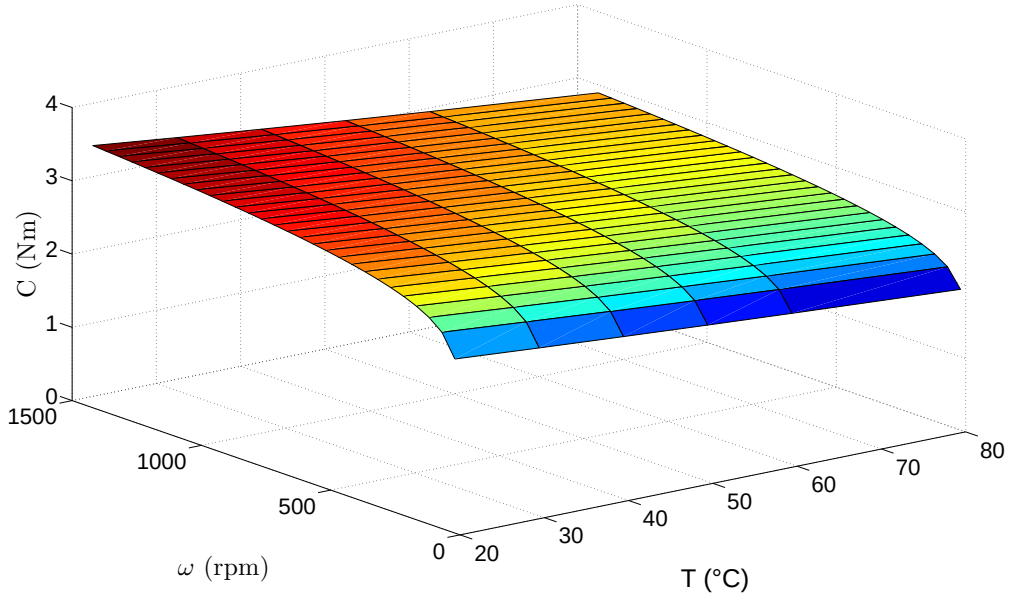

Figure 13. Torque fitting surface.

test. The temperature of the fluid at the beginning ($TC3_i$) and at the end ($TC3_f$) of each test was considered along with the energy dissipated E during the test, which is stated in Eq. 4 referring to a generic test time $\bar{t}$.

$$E(\bar{t}) = \int_0^{\bar{t}} C(t)\Delta\omega(t)\ \mathrm{d}t \tag{4}$$

The fluid temperature value during the test was supposed to vary, between its initial and final values, proportionally with the dissipated energy, neglecting any thermal transient. The updated temperature value T, referring to a generic test time $\bar{t}$, then resulted

$$T(\bar{t}) = TC3_i + \frac{E(\bar{t})}{E(t_f)}(TC3_f - TC3_i) \tag{5}$$

where $E(t_f)$ is the energy total energy dissipated at the end of each test. On the basis of the updated temperature values, the *MatLab Curve Fitting Tool* was used to find the parameters of the relationship defined by Eq. 3. The new fitting parameters are listed in Tab. 4.

Table 4. Fitting parameters.

A (Nm/rpm^n)	0.4146
n	0.1123
B (K^{-1})	410.6

The goodness of fit resulted enhanced as proven by the R-square index which resulted 0.9085.

5. SHEAR STRESS ASSESSMENT

In order to give a more general contribution, on the basis of the obtained results, the dependence of the shear stress on the temperature was estimated, with some simplifying hypotheses. The torque C is function of the speed difference $\Delta\omega$ and of the temperature T and, considering the clutch geometry shown in Fig. 1, is composed of two parts

$$C(\Delta\omega, T) = C_d(\Delta\omega, T) + C_c(\Delta\omega, T) \tag{6}$$

where C_d is the torque transmitted by the discoidal surface of the MR fluid and C_c is the one transmitted by the cylindrical surface.

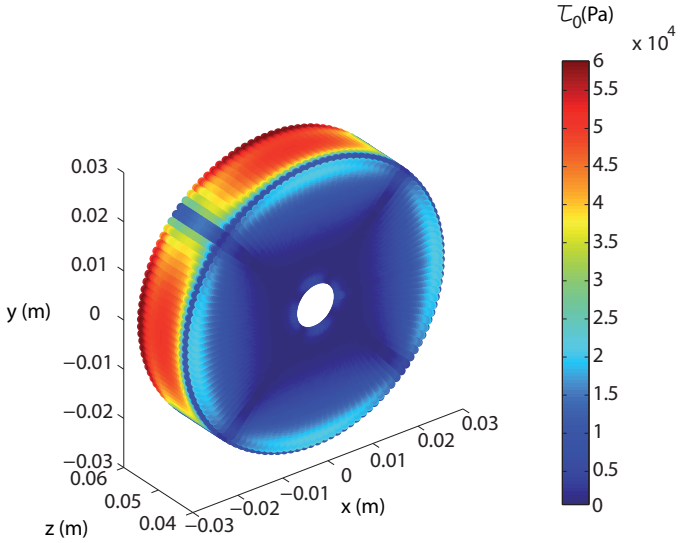

Figure 14. Computed yield stress distribution.

During the clutch design, finite element simulations were carried out [11] to obtain the distribution of the magnetic field and the shear stress τ_0 was then calculated on the basis of the formulation proposed by Carlson in [14] (Eq. 7)

$$\tau_0 = 271700\,\phi^{1.5239}\tanh\left(6.33\,10^{-6}\,H\right) \tag{7}$$

where ϕ is the volume particle fraction which is 0.4 [15] for the selected fluid, H is the magnetic field expressed in A/m computed at $T = 20^{\circ}\mathrm{C}$ and τ_0 results in Pa. Figure 14 shows the distribution of τ_0 in engaged condition. The simulations were used to compute the ratio α between C_d and C_c at room temperature ($T = 20^{\circ}\mathrm{C}$) and at yielding ($\Delta\omega = 0$)

$$\alpha = \frac{C_d(0, 20^{\circ}\mathrm{C})}{C_c(0, 20^{\circ}\mathrm{C})} = 0.122 \tag{8}$$

The obtained value proves the low contribution of the discoidal part due either to the geometry or to the low magnetic field; considering also the results reported by Sahin in [5] on MR greases, a low value of the magnetic field is expected to produce a fairly constant shear stress with respect to temperature and therefore

$$C_d(\Delta\omega, T) \simeq C_d(\Delta\omega) = \alpha C_c(\Delta\omega, 20^{\circ}\mathrm{C}) \tag{9}$$

The amount of torque due to the cylindric part of the MR meatus then is prevalent and, assuming α to be constant with respect to $\Delta\omega$, can be expressed as

$$C_c(\Delta\omega, T) = C(\Delta\omega, T) - \alpha C_c(\Delta\omega, 20^{\circ}\mathrm{C}) \tag{10}$$

The average shear stress in the cylindric portion of the meatus $\bar{\tau}(\Delta\omega, T)$ can finally be computed as

$$\bar{\tau}(\Delta\omega, T) = \frac{C_c(\Delta\omega, T)}{2\pi L R_m^2} \tag{11}$$

where L and R_m are the length and the mean radius of the cylindrical gap, respectively.

The average value of the shear stress on the cylindrical gap is plotted in Fig. 15 as a function of $\Delta\omega$ and T. This trend can not be considered as a precise estimation of the dependence of the

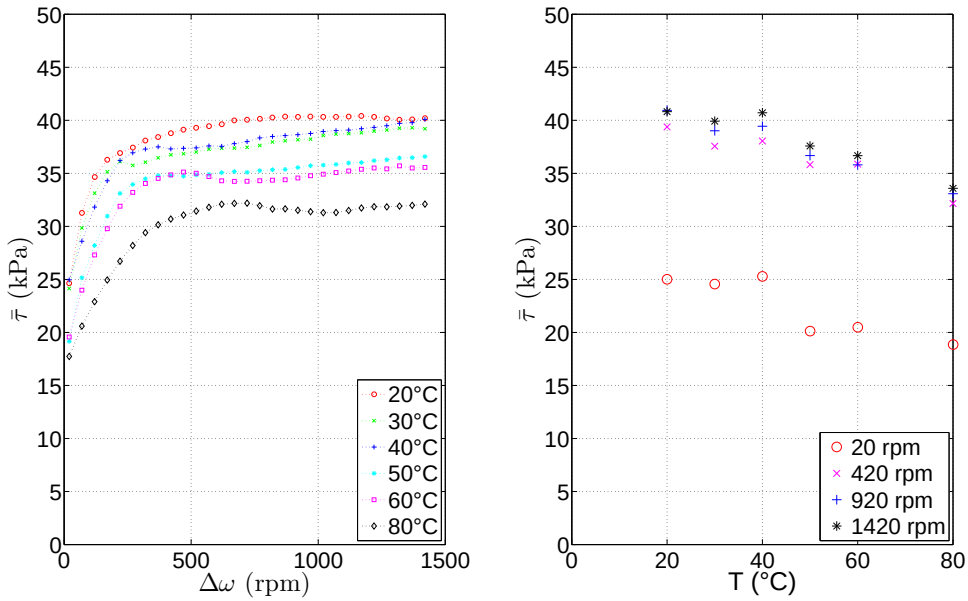

Figure 15. Average stress in the cylindrical gap function of relative speed and temperature.

fluid shear stress on temperature, due to the hypotheses made in the previous section and due to the non uniform distribution of τ_0 along the cylindrical gap as shown in Fig.14. However, it could be useful to estimate the performance of similar devices at different temperature values.

6. CONCLUSIONS

In the present paper the effect of temperature on the torque transmission characteristics of an MR clutch have been experimentally investigated.

A caulk oven with four heating elements was used to change the operating temperature of the clutch and three thermocouples were used to measure the temperature in three different positions on the clutch itself. Tests were performed on a dedicated bench in which the torque transmitted by the clutch was obtained in the temperature range (20 ^{o}C - 80 ^{o}C) as function of the relative speed between the input and output shaft. At 80 ^{o}C the transmitted torque reduced of about 20%, with respect to the torque measured at 20 ^{o}C. A power law and the Arrhenius law were found to satisfactorily fit the dependence on the relative speed and on the temperature, respectively.

In the final part of the work an approximate dependence of the yield stress of the MR fluid on the operating temperature is also obtained by some simplifying assumptions. Such results, for which no focused investigation was found on the technical literature, could be used to predict the operating capabilities of the developed device, as well as of similar devices, at different temperatures.

References

[1] F. Zschunke, R. Rivas and P. O. Brunn. Temperature Behavior of Magnetorheological Fluids. *Applied Rheology* 15(2), 116–121, 2005.

[2] C. Guerrero-Sanchez, A. Ortiz-Alvarado and U. S. Schubert. Temperature effect on the magneto-rheological behavior of magnetite particles dispersed in an ionic liquid. *Journal of Physics: Conference Series.* 149, 012052, 2009.

[3] C. W. Macosko. Rheology - Principles, Measurements and Applications *Wiley-VCH* 1994.

[4] W. Zhang, X. Gong, S. Xuan, W. Jiang. Temperature-Dependent Mechanical Properties and Model of Magnetorheological Elastomers. *Industrial and Engineering Chemistry Research* 50(11), 6704-6712, 2011.

[5] H. Sahin, X. Wang and F. Gordaninejad. Temperature Dependence of Magneto-rheological Materials. *Journal of Intelligent Material Systems and Structures.* 20(18), 2215–2222, 2009.

[6] F. Gordaninejad, D. G. Breese. Heating of magnetorheological fluid dampers. *Journal of intelligent material systems and structures.* 10(8), 634–645, 1999.

[7] R. Russo, M. Terzo. Design of an adaptive control for a magnetorheological fluid brake with model parameters depending on temperature and speed. *Smart Materials and Structures.* 20(11), 115003, 2011.

[8] G. Armenio, E. Bartalesi, F. Bucchi, A. Ferri, P. Forte, F. Frendo, R. Rizzo and R. Squarcini. Mechanical combustion engine driven fluid pump *EPO Patent.* 114251176.2-2423, 2011.

[9] F. Bucchi, P. Forte, A. Franceschini, F. Frendo Caratterizzazione sperimentale di prototipi di frizione magnetoreologica *41° convegno nazionale AIAS* Vicenza, 2012.

[10] F. Bucchi, P. Forte and F. Frendo. Design and experimental characterization of a permanent magnet magnetorheological clutch *Proceeding of ASME* ESDA Conference, Nantes, 2012.

[11] R. Rizzo, A. Musolino, F. Bucchi, P. Forte and F. Frendo. A fail-safe magnetorheological clutch excited by permanent magnets. Magnetic FEM analysis and Experimental Validation. *Journal of Intelligent Material Systems and Structures* Submitted, 2013.

[12] F. Bucchi, P. Forte, F. Frendo, R. Rizzo, A. Musolino. A fail-safe magnetorheological clutch excited by permanent magnets. Design and prototype testing. *Journal of Intelligent Material Systems and Structures* Submitted, 2013.

[13] F. Bucchi, P. Forte, F. Frendo, R. Squarcini. A magnetorheological clutch for efficient automotive auxiliary device actuation *Frattura ed Integrità Strutturale* 23, 62-74, 2013.

[14] J. D. Carlson MR fluids and devices in the real world *International Journal of Modern Physics B* 19 (7-9), 1463-1470, 2005.

[15] M. Schwartz Smart Materials *CRC Press - Taylor and Francis Group*, 2009.